UNLIMITED

CR115187

AD-A229 040

RSRE
MEMORANDUM No. 4375

ROYAL SIGNALS & RADAR
ESTABLISHMENT

ANALYSIS OF THE PERFORMANCE OF A SINGLE-AUXILIARY
SIDELOBE CANCELLER

Authors: I Day & A C Fairhead

RSRE MEMORANDUM No. 4375

DTIC
ELECTE
NOV 2 7. 1990
S B D

UNLIMITED

90 11 26 270

ROYAL SIGNALS AND RADAR ESTABLISHMENT

Memorandum 4375

TITLE: ANALYSIS OF THE PERFORMANCE OF A SINGLE-AUXILIARY
            SIDELOBE CANCELLER

AUTHORS: I Day and A C Fairhead

DATE: August 1990

SUMMARY

The geometrical approach to analysing the performance of simple sidelobe
canceller systems is illustrated. Systems with a single degree of freedom and
with a two-tap transversal filter are analysed. Throughout, examples are given
based on RSRE's BYSON antenna. These show that a single auxiliary channel
containing a two-tap transversal filter allows jamming arriving from any azimuth
to be nulled over the radar-signal bandwidth. More general results may be
deduced from the analysis.

THIS PAGE IS LEFT BLANK INTENTIONALLY

CONTENTS

THIS PAGE IS LEFT BLANK INTENTIONALLY

1 INTRODUCTION

Radars which use a directional receive beam can be rendered useless by interference received in the sidelobes of that beam. The sidelobe canceller (SLC) attempts to suppress such interference by subtracting from it an independent version which is identical in amplitude and phase. The version is obtained by receiving the interference in one or more auxiliary antennas and then appropriately adjusting its amplitude and phase to match that in the main channel. The arrangement with one auxiliary is shown in fig 1. The output can be considered to have been received by a composite antenna which has an angular response equal to the difference of the main antenna's response and a scaled and phased version of the auxiliary's angular response. The composite response will have a directional mainlobe virtually identical to that of the main antenna, but will also have a null in the direction of the interference.

Since the direction of interference cannot be known beforehand and since anyway it may change with time, the auxiliary phase and amplitude must be adjusted automatically. The appropriate settings are computed within the SLC from an adaptive algorithm based in principle on comparing the amplitude and phase of the two (or more) versions of interference entering the SLC. The computation part of the SLC is not shown in fig 1 because it is not the subject of this report. (algorithms for the adaptive spatial nulling of interference are fully described in the literature: see for example [1,2,3].) Rather than to study the algorithms themselves, which are intended to find the optimum setting (given the constraints of the SLC structure), it is easier and more instructive to consider what the optimum amplitude and phase setting would be if the interference were completely known. This report is intended to show that simple geometrical arguments can reveal the performance of certain SLC systems and that no adaptive-processing theory at all is required.

The simplest, single-auxiliary system is analysed in section 2. This has only one degree of freedom and can therefore perfectly null only a signal of one particular frequency arriving from one direction. Expressions are derived for the angular width and the frequency bandwidth of the null in the composite antenna's response. These allow us to decide over what angular and frequency-spread the SLC can be considered to cancel signals that arrive from a spread of directions or with a spread of frequency.

Throughout the report, examples are based on a system using RSRE's BYSON antenna with one auxiliary. Because of mechanical restrictions, this could not conform to the simplest theoretical model mentioned above. The extra features of the BYSON-type system are included in the analysis of section 2. The analysis guides the placement of the auxiliary horn to a position vertically above or below the centre of the main reflector. Nevertheless, the system would not cope at all angles with jamming that occupied a frequency band even only as wide as a typical radar-signal bandwidth (10 MHz).

We therefore investigate in section 3 the use of a simple transversal filter in the auxiliary channel: a method often suggested for improving bandwidth performance [4]. Using the same approach as before, simple geometrical arguments show how the transversal filter results in better performance; and again we are able to define the limits of the improvement that could be obtained in the BYSON system. For systems such as BYSON with large electrical dimensions, there is a definite upper limit on the delay in the transversal filter, which could be inconvenient in a digital implementation. Such conclusions as this are summarised in section 4. The wider implications of the results are also discussed in section 4.

2 ANALYSIS OF SLC WITH ONE DEGREE OF FREEDOM

2.1 Response of Simple Composite Antenna

We shall analyse the simple arrangement of fig 1 in order to establish the

procedures that will be used later for more realistic systems. To set up the SLC initially, we postulate that interference with angular frequency ω_j reaches the antennas at an angle θ_j to the normal. We consider that the SLC sets φ_j in order to cancel that interference (no auxiliary amplitude-adjustment is needed in this simplest model if we assume that both antennas have identical beam patterns). The phase difference between the interference in the two channels is $2\pi\delta/\lambda_j$ where δ is the difference between the paths from the source to each antenna, and λ_j is the wavelength of the interference. From fig 1, $\delta = d \sin \theta_j$.

$$\varphi_j = -\frac{\omega_j d}{c} \sin \theta_j \quad .$$

We wish to know the response of the resulting composite antenna as a function of frequency and direction. This is done effectively by postulating a test signal with variable direction θ and frequency ω, which produces signals s_1 and s_2 at the respective antennas; and then deriving the output $s(\theta, \omega)$ of the composite antenna. To simplify further, we assume both antennas are omnidirectional and that s_1 and s_2 have unit amplitude.

Let

$$s_1 = e^{j\omega t} \quad .$$

then

$$s_2 = e^{j(\omega t + \varphi)}$$

where

$$\varphi = \frac{\omega d}{c} \sin \theta .$$

Now

$$s_2' = e^{j(\omega t + \varphi + \varphi_j)}$$

$$= \exp\left\{ j\left[\omega t + \frac{\omega d}{c} \sin \theta - \frac{\omega_j d}{c} \sin \theta_j \right] \right\}$$

$$s = s(\theta, \omega) = \exp(j\omega t) \left[1 - \exp\left\{ j\left[\frac{\omega d}{c} \sin \theta - \frac{\omega_j d}{c} \sin \theta_j \right] \right\} \right] \quad (1)$$

However, we are only concerned with the power response $|s|^2$ of the composite antenna to the test signal.

$$|s|^2 = ss^* = 2 - 2\cos\left[\frac{\omega d}{c} \sin \theta - \frac{\omega_j d}{c} \sin \theta_j \right] \quad (2)$$

Note that this function will take value between 0 and 4. An arbitrary value of $|s|^2$ is taken as the limit below which the signal is considered to have been nulled. In this case, any value of $|s|^2 < 4/1000$ is taken to be part of the null. This value corresponds to one thousandth of the peak response power, indicating where cancellation is 30 dB or better.

2.1.1 Angular Width of the Null

To obtain the angular width of the null, $\Delta\theta$, we need to know the angle $\theta_j + \Delta\theta/2$ at the edge of the null (θ_j is assumed to be the centre of the null). At this angle,

$$|s|^2 = 2 - 2 \cos\left\{ \frac{\omega d}{c} \sin\left[\theta_j + \frac{\Delta\theta}{2}\right] - \frac{\omega_j d}{c} \sin\theta_j \right\} = \frac{4}{1000} \quad (3)$$

At the jamming frequency, ie. $\omega = \omega_j$, and after expanding $\sin(\theta_j + (\Delta\theta/2))$, (3) becomes

$$\frac{\omega_j d \Delta\theta}{2c} \cos\theta_j \approx 0.998,$$

$$\Delta\theta \approx \left| \frac{2c \cos^{-1}(0.998)}{\omega_j d \cos\theta_j} \right| \qquad (4)$$

The increase in null width $\Delta\theta$ with angle of incidence θ_j is to be expected because the projected length of the composite aperture decreases. Note also that $\Delta\theta$ is a function of d, ω_j and the nulling criterion (−30 dB in this case).

2.1.2 Frequency Bandwidth of the Null

To determine the frequency bandwidth of the null, Δf, rearrange (2) to obtain a factor $\omega - \omega_j$ in the argument of the cosine. In the direction of jamming, ie. when $\theta = \theta_j$,

$$|s|^2 = 2 - 2\cos\left\{ \frac{d}{c} \left[\omega - \omega_j\right] \sin\theta_j \right\}.$$

At the edge of the null,

$$2 - 2\cos\left[\frac{\pi \Delta f d}{c} \sin\theta_j\right] = \frac{4}{1000}$$

$$\Delta f = \left| \frac{c \cos^{-1}(0.998)}{\pi d \sin\theta_j} \right| \qquad (5)$$

Note that a null at boresight ($\theta_j = 0$) has infinite bandwidth, and that as θ_j increases in either direction, the bandwidth decreases. This is because the path difference increases with angle of incidence. The phase−shift of a signal with angular frequency ω due to a path length of l is $-\omega l/c$, which becomes more sensitive to changes in frequency as l increases. Although the phase−shift φ_j can be set so that jamming signals of frequency ω_j are in phase in the main and auxiliary channels, jamming components with a frequency different from ω_j will not be as effectively cancelled as l increases.

3

2.1.3 The "phase-difference" Surface

An important quantity for understanding the frequency-dependent nulling of broadband jamming at any particular angle θ_j is the surface

$$\delta\gamma(\theta_j, \delta\omega) = \langle s_2(\theta_j, \omega_j + \delta\omega) - \langle s_1(\theta_j, \omega_j + \delta\omega)$$

$$= \langle s_2(\theta_j, \omega_j + \delta\omega) + \gamma_j - \langle s_1(\theta_j, \omega_j + \delta\omega) \qquad (6)$$

Now, $\langle s_2 - \langle s_1 = (\omega_j + \delta\omega)t + (\omega_j + \delta\omega)\dfrac{d}{c}\sin\theta_j - (\omega_j + \delta\omega)t$

$$= (\omega_j + \delta\omega)\dfrac{d}{c}\sin\theta_j$$

is simply the frequency-dependent phase difference between the auxiliary and main channels for broadband jamming at direction θ_j and centred on ω_j. The addition of γ_j, as in (6), merely sets this to zero at ω_j.

$$\delta\gamma(\theta_j, \delta\omega) = (\omega_j + \delta\omega)\dfrac{d}{c}\sin\theta_j - \dfrac{\omega_j d}{c}\sin\theta_j$$

$$= \dfrac{\delta\omega d}{c}\sin\theta_j$$

Even after the phase-shifter, a frequency-dependent phase shift with gradient $dc\sin\theta_j$ remains. Jamming components with this phase difference are subtracted from one another in the SLC. The phase-difference surface for $d = 2.2m$ is shown in fig 2.

Simple phasor arithmetic can show that the criterion for cancelling by 30 dB or more a jamming component with equal amplitude in the main and auxiliary channels is that the phase difference $|\delta\gamma|$ should not exceed 3.6°. The linear slope of the surface $\delta\gamma$ parallel to the frequency axis at the particular angle of jamming θ_j therefore determines over what range of $\delta\omega$ the criterion is satisfied. Fig 2 illustrates what was determined in section 2.1.2: that for jamming close to boresight (θ_j small), the surface slopes gently with frequency, so the bandwidth of the null is wide; for jamming further away from boresight, the slope increases, narrowing the bandwidth of the null.

2.2 A Practical System

The system considered so far does not represent a real one consisting of a main reflector antenna (eg BYSON) with a horn at its focus, and a separate auxiliary horn. Fig.3a is a plan view of a practical system, showing the extra distance in the horizontal plane that the signal must travel to reach the main horn via the reflector (Here, the reflector is modelled as a plane for simplicity.) The extra distance, l_1, is a function of angle of incidence. By rearranging the geometry, as in fig 3b, it can be shown that $l_1 = 2h\cos\theta$, where h is the distance between main horn and reflector. In the schematic, fig 4, it is more convenient to model l_1 as a negative path length in the auxiliary channel, even though it actually occurs as an extra, positive path length in the main channel. As will be shown in section 2.2.2, l_1

4

severely degrades the bandwidth over which nulling occurs unless a compensating delay-line of length l_2 is also included in the auxiliary channel.

As before, the phase shift φ_j is set to the difference in phase between s_1 and s''_2, which are the input signals to the SLC for an initial signal with angular frequency ω_j and incident at θ_j (for which $l_1 = 2h \cos \theta_j$). Thus

$$\varphi_j \;=\; - \frac{\omega_j d}{c} \sin \theta_j + \frac{\omega_j}{c} \left[l_2 - 2h \cos \theta_j \right].$$

Then, for a test signal varying in ω and θ (for which $l_1 = 2h \cos \theta$),

$$s_1 \;=\; e^{j\omega t} \;;$$

$$s'_2 = \exp\left\{ j\left[\omega t + \frac{\omega d}{c} \sin \theta - \frac{\omega}{c}\left(l_2 - 2h\cos\theta \right) + \varphi_j \right]\right\}$$

Substituting for φ_j,

$$s'_2 = \exp\left\{ j\left[\omega t + \frac{d}{c}\left(\omega\sin\theta - \omega_j \sin\theta_j \right) - \frac{l_2}{c}\left(\omega - \omega_j \right) \right.\right.$$

$$\left.\left. + \frac{2h}{c}\left(\omega\cos\theta - \omega_j \cos\theta_j \right) \right]\right\}$$

Following a similar procedure to that in section 2.1, we obtain the power response of the system

$$\left| s(\theta,\omega) \right|^2 \;=\; 2 - 2\cos\left\{ \frac{d}{c}\left(\omega\sin\theta - \omega_j\sin\theta_j \right) - \frac{l_2}{c}\left(\omega - \omega_j \right) \right.$$

$$\left. + \frac{2h}{c}\left(\omega\cos\theta - \omega_j\cos\theta_j \right) \right\}$$

2.2.1 Angular Width of the Null

The same procedure that was used in section 2.1.1 gives

$$\Delta\theta \;=\; \left| \frac{2c\,\cos^{-1}(0.998)}{\omega_j(d\cos\theta_j - 2h\sin\theta_j)} \right|$$

Computed results for a system using BYSON are shown as a dotted line in Fig 5. For comparison, results computed from (4) are shown as a solid line. The null tends to be narrower in the practical system because of l_1, which makes the effective

5

aperture of the system in fig 3a wider than that of the system in fig 1 at angles away from boresight. Note from (8) that $\Delta\theta$ is not affected by the choice of l_2.

2.2.2 Frequency Bandwidth of the Null

Following the procedure in section 2.1.2, set $\theta = \theta_j$ in (7), so that in the direction of jamming,

$$|s|^2 = 2 - 2 \cos\left\{ \frac{\omega - \omega_j}{c} (d\sin\theta_j + 2h\cos\theta_j - l_2) \right\}$$

At the edge of the null,

$$2 - 2\cos\left\{ \frac{\pi\Delta f}{c} (d\sin\theta_j + 2h\cos\theta_j - l_2) \right\} = \frac{4}{1000}$$

$$\Delta f = \left| \frac{c \cos^{-1}(0.998)}{\pi(d\sin\theta_j + 2h\cos\theta_j - l_2)} \right| \qquad \qquad \text{(9)}$$

The solid line in fig 6 is a result for a system based on BYSON with l_2 set to zero. This demonstrates that, without compensation for l_1, the bandwidth of the null is insufficient for cancelling broadband jamming, which will have a spectrum at least as wide as the signal-bandwidth of the radar (say 10 MHz). The reason for this is that l_1 is long, many times the wavelength of incoming radiation, so the phase-shift it imparts to the different frequency components of the jamming is a sensitive function of the angular frequency ω. The phase-shifter setting τ_j can only ensure perfect cancellation of the central component ω_j.

It can be seen from (9) that nulling bandwidth at any angle θ_j is a function of l_2 which can, in fact, be made infinite by choosing $l_2 = d\sin\theta_j + 2h\cos\theta_j$. However, lacking any prior knowledge of specific jammer directions, or any other guidance, we might choose l_2 to compensate completely for l_1 at boresight. (The main antenna probably rotates anyway, in which case, incidentally, the auxiliary horn should be mounted on the same rotating platform.) Then $l_2 = 2h$ and

$$\Delta f = \left| \frac{c \cos^{-1}(0.988)}{\pi\left\{d\sin\theta_j + 2h(\cos\theta_j - 1)\right\}} \right|$$

A plot of Δf vs θ_j for the BYSON system (d = 2.2m, 2h = 12.24m) is shown as the dotted line in fig 6.

Alternatively, since l_1 shortens as the angle of incidence increases in either direction from boresight, we might choose l_2 to be short as possible while still allowing say 10 MHz nulling bandwidth for all angles around boresight. This would be expected to provide 10 MHz nulling over the widest possible sector. For a system based on BYSON, it turns out that $l_2 = 2h - 0.43$ metres. The dashed curve in fig 6 is a plot of Δf with this value of l_2. Comparison with curve 2 shows that the sector over which 10 MHz nulling bandwidth is maintained is wider, at around 51°.

However, a point to notice about (9) and fig 6 is that the response of the system illustrated in fig 3a is not symmetrical about boresight, $\theta_j = 0$. The reason is that the system itself is not symmetrical about boresight: the auxiliary is displaced

6

to one side.   Such displacement is often assumed in an SLC but there seems to be
no good reason for it.   We therefore consider a system in which the auxiliary horn
is positioned in the vertical plane of boresight.

2.3   Practical System with Symmetry

Fig 7a shows a plan view of the arrangement. The auxiliary horn is positioned
behind the main horn by a distance p.   A side view would show it also displaced
vertically to avoid obscuring the main horn from the reflector, but we are only
concerned with a horizontally-planar system for simplicity.

As before, by rearranging the geometry as in fig 7b, it can be shown that the
path length to the main horn is longer than that to the auxiliary by an amount
$l_1 = (2h - p)\cos\theta$.   Given that l_1 is different from before, fig 4 is still a valid
model for the symmetrical system.

The phase-shifter setting φ_j will also be a different function of jamming
direction θ_j, because the auxiliary is no longer set to one side.

$$\varphi_j = \frac{\omega_j(l_2 - l_1)}{c} = \frac{\omega_j}{c}\left\{l_2 - (2h - p)\cos\theta_j\right\}.$$

Then

$$s_2'(\theta,\omega) = \exp\left\{j\left[\omega t - \frac{\omega(l_2 - l_1)}{c} + \varphi_j\right]\right\}.$$

Substituting for l_1 and φ_1.

$$s_2'(\theta,\omega) = \exp\left\{j\left[\omega t - \frac{\omega}{c}\left\{l_2 - (2h - p)\cos\theta\right\}\right.\right.$$

$$\left.\left. + \frac{\omega_j}{c}\left\{l_2 - (2h - p)\cos\theta_j\right\}\right]\right\}$$

$$= \exp\left\{j\left[\omega t - \frac{\omega - \omega_j}{c}l_2 + \frac{2h - p}{c}(\omega\cos\theta - \omega_j\cos\theta_j)\right]\right\}$$

Again, following the same procedure as in section 2.1, the power response of
the system is

$$\left|s(\theta_j,\omega)\right|^2 = 2 - 2\cos\left\{\frac{2h - p}{c}(\omega\cos\theta - \omega_j\cos\theta_j) - \frac{l_2}{c}(\omega - \omega_j)\right\}$$

(10)

2.3.1   Angular Width of the Null

The same procedure that was used in section 2.1.1 gives

$$\Delta\theta \approx \left| \frac{-2c \cos^{-1}(0.998)}{(2h-p)\omega_j \sin\theta_j} \right| \text{ radians} \tag{11}$$

$$\approx \left| \frac{0.01}{\sin\theta_j} \right| \text{ degrees, with the BYSON parameters } (p = 1.24).$$

$\Delta\theta$ for the symmetrical system is plotted as the dashed line in fig 5. The above approximations break down for θ_j within about $\frac{1}{4}^\bullet$ of boresight. Exact calculation shows that the angular width of the BYSON system at boresight is $1.5^\bullet$. It can be seen from (11) that $\Delta\theta$ does not depend on l_2.

2.3.2 Frequency Bandwidth of the Null

The same procedure as in section 2.1.2 gives

$$\Delta f = \left| \frac{c \cos^{-1}(0.998)}{\pi\left\{(2h-p)\cos\theta_j - l_2\right\}} \right| . \tag{8}$$

Since $l_1 = (2h-p)\cos\theta_j$ shortens as the angle of incidence θ_j increases in either direction from boresight, l_2 should be made as short as possible while still allowing 10MHz nulling bandwidth at boresight. Then $l_2 = 2h-p-0.6$ metres. Fig 8 is a plot of Δf with the BYSON parameters and this value of l_2. It can be seen that a *nulling bandwidth of at least 10 MHz is achieved* at all angles within $2^{-\bullet}$ of boresight. Although this is a slightly wider sector than was provided by the unsymmetrical system considered in section 2.2 (the dashed curve in fig 6), it can be seen by comparing the denominators of expressions (9) and (12) for practical systems with that of (5) for the simple system that the bandwidth of the null is reduced by separation of the main and auxiliary horns and by other physical features that produce differences in path length from the jammer to the two horns. These features cannot usually be reduced indefinitely, and it has been demonstrated above that inserting compensating lengths of cable increases the bandwidth only over a certain angular sector. In the next section we examine an alternative method, based on providing an extra degree of freedom to match the group delay of the auxiliary channel to that of the main channel.

The dimension p in fig 7a, however, may be under the control of the SLC designer, and therefore the factor (2h-p) that features in the above analyses. That factor should be minimised in order to minimise the path-length difference between the two channels and to maximise the nulling bandwidth. It could probably be reduced to h, in which case the auxiliary horn would be directly above or below the main reflector; but not much beyond that. Nevertheless, this would double the nulling bandwidth achieved at larger angles from boresight compared with that in fig 8. Using (12) it can be shown that the angle up to which 10 MHz nulling bandwidth is achieved is increased to $37^\bullet$.

3 SLC USING A TRANSVERSAL FILTER

3.1 Introduction

The reason that the system considered in section 2.3 can null signals over a 10 MHz bandwidth only if they arrive from within $27^\bullet$ of boresight can be seen from fig

9.   This shows the surface, introduced in section 2.1.3, of the phase difference $\delta\varphi$ between the frequency components of jamming in the main channel and in the auxiliary after the phase shifter, for angles of arrival θ_j of the jamming between $-80°$ and $+80°$ and for components with frequency offset δf between ± 5 MHz of ω_j.

$$\delta\varphi(\theta_j, \delta\omega) \;=\; <s_2'(\theta_j, \; \omega_j + \delta\omega) \;-\; <s_1(\theta_j, \; \omega_j + \delta\omega)$$

$$=\; \frac{-\delta\omega}{c}\left\{ l_2 - (2h - p)\cos\theta_j \right\} \quad (\text{from section } 2.3) \quad (13)$$

As before, at any angle θ_j, $\delta\varphi$ is a linear function of frequency. The group-delay difference δD between channels is

$$\delta D \;=\; -\left[\frac{\partial(\delta\varphi)}{\partial\,\delta\omega} \right]_{\theta_j} \;=\; \frac{l_2 - (2h - p)\cos\theta_j}{c}$$

(This is simply the difference in path lengths of the two channels, divided by the velocity of propagation.)

A single phase-shifter cannot change the phase-slope or group-delay of the auxiliary channel, and cannot compensate for the group-delay difference δD. In order to improve the bandwidth performance of the system, we must replace the phase shifter with a filter that can adjust its phase slope to be the opposite of that of $\delta\varphi$ at the angle of jamming θ_j. The whole point of any "processing" in the auxiliary channel is to mirror the function $<s_2(\theta_j,\omega) - <s_1(\theta_j,\omega)$ for any given θ_j, so that $\delta\varphi(\theta_j,\delta\omega) \approx 0$ over the signal bandwidth of the radar. (In practice, it should also attempt to match $|s_2(\theta_j,\omega)|$ with $|s_1(\theta_j,\omega)|$, but for simplicity in this report we assume that $|s_2| = |s_1| = 1$.)

A filter can only produce a negative phase-slope, however, so before it can be applied, the phase-difference surface in fig 9 must be rotated about the θ_j axis so that all slopes parallel to the frequency axis are positive within the sector over which wideband nulling is required.   Simply changing the group-delay difference δD will achieve this.   A positive slope of $\delta\varphi$ parallel to the frequency axis requires the secondary channel path-length to be shorter than that of the main, which is $(2h-p)$ $\cos\theta$.   Therefore, if wideband nulling is required for all angles within θ_{jmax} of boresight, l_2 must not be greater than $(2h - p)\cos\theta_{jmax}$ metres in length. This may be shorter than was found permissible for the single phase-shifter system considered in section 2.3, and could result in a path-length mismatch for small θ_j that would severely degrade the nulling bandwidth of such a system.   Here, however, we are relying on the filter to be able to insert the necessary group-delay to make up the difference.   Substituting $l_2 = (2h - p)\cos\theta_{jmax}$ in (13), the rotated phase-difference surface becomes

$$\delta\varphi(\theta_j, \delta\omega) \;=\; -\frac{\delta\omega}{c}(2h - p)(\cos\theta_{jmax} - \cos\theta_j). \qquad (14)$$

Within the sector $\pm\theta_{jmax}$ of interest, the maximum path-length difference now occurs at boresight, $\theta_j = 0$, for which the phase difference as a function of frequency is

$$\delta\varphi(0, \delta\omega) \;=\; -\frac{\delta\omega}{c}(2h - p)(\cos\theta_{jmax} - 1).$$

Nulling of all jamming components within some bandwidth $\pm\delta\omega_{max}$ will be required. The maximum phase difference that the filter must correct is therefore.

$$\delta\varphi_{max} = \delta\varphi(0, \pm\delta\omega_{max}) = \pm\frac{\delta\omega_{max}}{c}(2h - p)(1 - \cos\theta_{jmax})$$

$$(15)$$

An example of a rotated phase-difference surface for the BYSON system is shown in fig 10. To allow wideband nulling within a $\pm60°$ sector, l_2 is made $(2h-p)/2$ metres in length. It can be seen that the phase-slope with frequency is zero at $\pm60°$ and is positive elsewhere, being maximum at boresight. The maximum phase differences $\pm\delta\varphi_{max}$ over a 10 MHz band are $\pm32°$. For other sectors $\pm\theta_{jmax}$ of interest, $\delta\varphi_{max}$ over a 10 MHz bandwidth is plotted in fig 11.

A transversal filter is the most convenient way of synthesizing any required phase response. We shall limit our attention to the simplest type, shown in fig 12. This has just two coefficients or adjustable "weights" W_0 and W_1, and a fixed line producing delay τ. The weights are not just phase-shifters, but are generally complex, adjustable in both gain and phase-shift. The question to be answered is what settings of W_0, W_1 and τ optimise nulling performance. It should be remembered that we are not concerned here with the mechanisms by which such weights are set (i.e the adaptive algorithms), but only whether it is possible to set them and τ in such a way as to increase the cancellation bandwidth above that which can be achieved with a single phase-shifter.

3.2 Theory of Transversal Filter

The transversal-filter literature is not very helpful for this application because it is generally concerned with achieving a specified amplitude rather than phase-response. The resulting phase-response is only a by-product of the design procedures described. Fortunately, the simple filter of fig 12 is easy to analyse.

In an SLC, the filter essentially has two functions, and these are best illustrated by redrawing it as in fig 13. The phase-shift in W'_0 does a similar job to that in the systems considered in section 2, matching the phase of jamming at ω_j in the main and auxiliary channels. The second part of the filter produces a variable phase slope with frequency, by adding in a delayed version of the jamming components. The relative phase of these components has a negative linear slope fixed by τ. By adjusting the amplitude gain of W'_1, however, the amount of these components that is added to those coming directly through the second part of the filter can be varied. In this way, the phase slope of the resultant components, although nonlinear with frequency, can be varied in principle to any negative value. However, the addition of components whose relative phase varies with frequency gives them a frequency-dependent power spectrum. Since they are to be subtracted from those in the main channel, which have a flat power spectrum in our simple model, their spectrum must not vary by more than one thousandth of its peak power across the signal bandwidth of the radar if 30 dB nulling of all of them is to be achieved. This constraint limits the maximum phase-slope possible with a transversal-filter system.

In order to decide what the optimum settings are, we must first derive expressions for the output of the second part of the filter shown in fig 13. Consider a signal $s_{in} = e^{j\omega t}$. The output consists of two terms corresponding to the two paths by which input reaches output.

10

$$s_{out} = e^{j\omega t}(1 + W_1' \, e^{-j\omega\tau}) \ .$$

Let $W_1' = A_1 e^{j\varphi_1}$, where A_1 is positive real.

Then $s_{out} = e^{j\omega t}\left[1 + A_1 e^{j(\varphi_1 - \omega\tau)}\right]$.

That the output consists of two components is well illustrated by the phasor diagram, fig 14. The angle of the second component is a function of input frequency ω, with gradient $-\tau$. This is responsible for the change of phase with frequency of the resultant.

The output power is

$$\left|s_{out}\right|^2 = s_{out} s_{out}^* = 1 + A_1^2 + 2A_1 \cos(\omega\tau - \varphi_1) \ . \tag{16}$$

The phase of the output, $<s_{out}$, is obtained from fig 14 using the sine rule.

$$\frac{\sin(\varphi_1 - \omega\tau)}{\left|s_{out}\right|} = \frac{\sin(<s_{out})}{A_1} \ .$$

$$<s_{out} = \sin^{-1}\left\{\frac{A_1 \sin(\varphi_1 - \omega\tau)}{\sqrt{1 + A_1^2 + 2A_1 \cos(\omega\tau - \varphi_1)}}\right\} \tag{17}$$

This is a function of frequency, as required, which can be varied with the parameters A_1, φ_1 and τ. We now investigate constraints on the response s_{out}, to find the optimum values of these parameters.

3.3 Choice of Parameters

Since the output power-response of the filter (16) is symmetrical about its peak at $\omega = \varphi_1/\tau$, we could choose $\varphi_1 = \omega_j\tau$ to put the peak response at the centre jamming-frequency ω_j. This effectively lines up the two component phasors in fig 14 at band-centre. Then, from (16) and (17),

$$\left|s_{out}\right|^2 = 1 + A_1^2 + 2A_1 \cos(\delta\omega\tau) \tag{18}$$

and $<s_{out} = \sin^{-1}\left\{\dfrac{A_1 \sin(-\delta\omega\tau)}{\sqrt{1 + A_1^2 + 2A_1 \cos(\delta\omega\tau)}}\right\}$ \qquad (19)

11

The phase transfer-function $<s_{out}$ must be capable of mirroring the slope of a phase-difference surface such as in fig 10 for any particular θ_j: it must be as nearly linear as possible, zero at $\delta\omega = 0$ and adjustable from zero to $\pm\delta\varphi_{max}$ respectively of the frequency band of interest. ($\delta\varphi_{max}$ is defined in (15).) Adjustment of the maximum phase-transfer angle at the band-edge is achieved by varying A_1 between zero and some value A_{1max}. From fig 14, it is clear that a required $<s_{out}$ at frequency $\delta\omega$ can be achieved by different combinations of A_1 and τ. We show now, however, that there is a definite upper limit to the value of τ that will allow a range of phase-transfer functions to be achieved with acceptable power-transfer functions as well.. This maximum value, τ_{max}, results in the largest possible spread of phase-transfer functions and therefore in jamming being nulled over the largest possible sector.

The power-transfer function (eqn 18), if A_1 is non-zero, decreases symmetrically with frequency offset $\delta\omega$ (from ω_j) either side of zero. For the SLC to suppress all frequency components of jamming within the signal bandwidth by 30 dB or more, the amplitude response of the auxiliary filter at the edge of the band must not be less than $1 - \surd 0.001$ or 0.97 of that at the centre. The diagram of fig 15, which is based on the phasor diagram, fig 14, is useful for investigating the response of the filter with various combinations of A_1 and τ. The circle with radius $1 + A_1$ represents the peak amplitude response of the filter whatever the value of A_1. (The point with absolute value 1 will therefore change position on the real axis as A_1 is varied.) That with radius $(1 - \epsilon)(1 + A_1)$ represents the minimum acceptable amplitude response (for nulling of at least 30 dB, $\epsilon = \surd 0.001$). For a particular combination of A_1 and τ, the tip of the phasor s_{out} should stay between the two circles as ω varies. It should stay there, furthermore, once τ is fixed at τ_{max} and A_1 is subsequent varied to allow jaming from different directions to be nulled.

Consider the phasors shown to represent conditions at the edge of the band, where $\delta\omega = -\delta\omega_{max}$. s_{out} must have the same phase as the band-edge component of jamming from a particular direction. Now consider the isosceles triangle with two sides of length A_1. Its apex angle, $-\delta\omega_{max}\tau$, depends only on $|s_{out}|$ relative to its peak value $1 + A_1$ and on $<s_{out}$. In the position shown, with minimum acceptable $|s_{out}|$ and with the base of the triangle forming a tangent to the inner circle, the apex angle is smaller than for any other angle of s_{out}: although if A_1 were to be increased, to increase $|s_{out}|$ but keep $<s_{out}$ constant, the apex angle would decrease further. For the situation shown, therefore, the maximum permissible apex angle is

$$- \delta\omega_{max}\tau = \pi - 2\sin^{-1}(1 - \epsilon)$$

Even if a larger $<s_{out}$ at band-edge is required for some angles of jamming, τ must not be increased beyond

$$\tau_{max} = \frac{\pi - 2\sin^{-1}(1 - \epsilon)}{- \delta\omega_{max}} \tag{20}$$

otherwise $|s_{out}|$ at the angle $<s_{out}$ shown would be unacceptably low however large A_1 was made. Equation 20 shows, surprisingly, that τ_{max} depends on no parameters of the system apart from the bandwidth and the nulling criterion for the edge of the band. A plot of τ_{max} vs nulling criterion for a 10 MHz bandwidth system is given in fig 16.

With the value of τ_{max} determined by (20), the locus of the tip of s_{out} at band-edge follows the tangent to the inner circle shown in fig 16 as A_1 is varied. With A_1 at its largest practicable value (assuming this is $>> 1$), $(<s_{out})_{max} \approx -\delta\omega_{max}\tau_{max}$.

This is the largest phase-shift that the filter can produce at band-edge, and thus determines the angular sector over which 10MHz-bandwidth nulling of jamming can be achieved. Using (15),

$$- \delta\omega_{max}\tau_{max} \approx \delta\varphi_{max} = \frac{\delta\omega_{max}}{c} (2h - p)(1 - \cos\theta_{jmax}).$$

$$\therefore \quad \theta_{jmax} = \cos^{-1}\left[1 - \frac{\tau_{max}c}{2h - p}\right].$$

Unlike τ_{max}, θ_{jmax} is affected by the dimensions of the system. The fundamental relationship for the 2-tap transversal-filter SLC system is obtained by substituting for τ_{max} from (20). This gives

$$\theta_{jmax} = \cos^{-1}\left\{1 - \frac{c[\pi - 2\sin^{-1}(1 - \epsilon)]}{\delta\omega_{max}(2h - p)}\right\} \tag{21}$$

which is the relationship between the nulling criterion and the angular sector over which that criterion is satisfied. A plot of θ_{jmax} vs the criterion for nulling over a 10 MHz bandwidth with the BYSON system is given in fig 17. It shows that for 30 dB of nulling, $\theta_{jmax} = 56$ degrees, which is double that of the system without the transversal filter considered in section 2.3. If the factor 2h-p were reduced to h, as recommended in section 2.3.2, θ_{jmax} would increase to 78°, defining a sector that covers practically the whole of real azimuth.

Having fixed τ and adjusted A_1 so that the amplitude response of the filter is sufficiently flat across the band, we must check that the phase response is sufficiently linear with these parameters. The departure from linearity is given by subtracting the linear term from $<s_{out}$ in (19). It is not easy to analyse, but numerical computations show that it is negligible for all likely values of A_1 and τ. The amplitude-response requirements therefore appear to be a tighter constraint on the filter parameters than the phase-response requirements.

This completes the investigation of transversal-filter behaviour. We have not set out to develop a design procedure because the weights would be adjusted automatically by the adaptive algorithm. We have merely investigated how to set τ and over what angular sector and bandwidth the system should then achieve nulling. We finish this section by discussing the implications of setting τ.

In an analogue SLC system, where the signals are continuous in time, the delay τ would be produced simply by a delay line. In a digital system, however, signals are discrete in time, and only valid at the sampling times. Fig 16 shows that τ should generally be shorter than the sampling period, which would be around $\pi/\delta\omega_{max}$ (i.e 50ns for a 10 MHz bandwidth) to satisfy the Nyquist criterion. It would be most convenient if τ could be made equal to the sampling period, so that the filter would consist simply of adding together weighted, adjacent samples. Unfortunately, such a delay produces a phase-shift $\delta\omega\tau$ of 180° for signals of frequency-offset $\pm \delta\omega_{max}$ from band-centre. But, rearranging (20),

$$1 - \epsilon = \sin\left[\frac{\pi - \delta\omega\tau}{2}\right]$$

which for $\delta\omega\tau = \pi$ radians is zero. $(1 - \epsilon)$ is the radius of the inner circle in fig 15, and a value of zero implies that at some jamming direction, no cancellation at all is achieved at the edge of the band. This is confirmed by fig 16. The fact that the direction at which the poorest cancellation occurs may be outside real space if the electrical dimensions of the system were small is beyond the scope of this report.

A polar diagram such as in fig 18 could be used to investigate whether particular values of τ in a particular system would allow adequate nulling to be achieved over an adequate real sector. It is based on fig 15. Radial lines are drawn at various angles representing the maximum phase-shift $\delta\varphi_{max}$ required at the edge of the band for various directions θ_j of jamming. Their angles are calculated from (15) and are particular to the system being considered. Those shown are for BYSON. They represent a mapping of real azimuth from boresight of the system onto the polar diagram. Next, a straight line is drawn from the edge of the diagram at 0° to the edge of the diagram at angle $\delta\omega_{max}\tau$ (for τ corresponding to the period between Nyquist samples, this angle would be 180°). The line shown corresponds to the period between samples taken at twice the Nyquist rate. At any point along the line, the cancellation at band-edge and the azimuth at which that cancellation would occur can be read off.

4 DISCUSSION AND CONCLUSIONS

This report has aimed to illustrate some methods by which the performance of an SLC system can be analysed. The methods are based on simple geometry, not on adaptive-processing theory, but nevertheless allow the performance of particular systems to be predicted and the effects of parameter-variation to be studied.

The simplest SLC consists of a main antenna and a single auxiliary with adjustable gain and phase-transfer, i.e with one complex degree of freedom. Gain-control considerations may be neglected by considering that both antennae have identical beam patterns. In a real system, the auxiliary gain would be adjusted to match that of the main antenna in the direction of jamming. (It is not sensible to consider this system nulling more than one jammer.) The phase-shifter setting has more effect on the performance of the SLC and this may, at least to a first approximation be separated from that due to the gain setting. The angular width over which cancellation is effective is of interest because, for example, a near-field point source such as might be used for testing the SLC appears to occupy a sector of the far-field. Of even more interest is the frequency bandwidth over which cancellation is effective. The SLC should be capable of jamming over the signal bandwidth of the radar. Expressions have been derived for the angular width and frequency bandwidth of the null. The surface of phase-difference between the various frequency-components of jamming in the main and auxiliary channels as a function of their frequency and the direction of jamming ilustrates why the nulling bandwidth is limited, particularly for jamming from directions away from boresight.

A real system in which the main antenna consists of a reflector with a horn at its focus does not conform to the simplest SLC model. The considerable path-length difference between main and auxiliary channels due to the extra distance to and from the reflector has a severe effect on bandwidth performance. A compensating delay-line must be inserted in the auxiliary channel. The modified expressions for angular width and bandwidth of null show, however, that this system, which commonly has the auxiliary to one side of the boresight line of the main antenna, suffers from asymmetrical performance either side of boresight.

A symmetrical system should have the auxiliary in the vertical plane of boresight, but displaced from the centre line to avoid obscuring the main reflector. The horizontal distance between main and auxiliary horns may be under the control of the SLC designer, in which case the best practicable position for the auxiliary horn is directly above or below the main reflector. Expressions have been derived for the angular width and bandwidth of the null. The compensating delay-line in the auxiliary channel should be made as short as possible while still allowing adequate bandwidth at boresight. This arrangement maintains the required bandwidth over the largest possible sector for an SLC system with one degree-of-freedom. For a system based on BYSON, 10 MHz nulling bandwidth could be maintained for all angles within 27˚ of boresight, or 37˚ if the auxiliary could be positioned as recommended above.

Bandwidth performance remains limited, however, by the large dimensions of the system that are beyond the SLC-designer's control. The phase-difference surface shows that it can be improved by using a transversal filter in the auxiliary channel which can adjust its phase-transfer as a function of frequency. (The adaptive processor would make the appropriate adjustment.) The simplest transversal filter has just two complex degrees of freedom, or weights. One of these adjusts the gain and phase-transfer of the auxiliary channel to match those of the main channel at the centre jamming-frequency. The other adjusts the relative phase of other jamming frequencies to match that of those in the main channel.

Nulling bandwidth is still limited, however, not so much by the small remaining mismatch of phase between jamming components in the main and auxiliary channels, but more by the fact that the amplitude response of the filter rolls off towards the band-edges for most settings of the weights. If a certain minimum cancellation is to be maintained across the band for all directions of jamming within a sector round boresight, then the intertap delay in the filter cannot exceed a certain value. An expression has been derived for the maximum permissible intertap delay, which shows it to depend on no parameters of the system apart from the bandwidth required and the minimum acceptable nulling over that bandwidth. The values obtained are generally much less than the period between Nyquist samples, making an analogue implementation of the filter more practicable than a digital one. It might be possible to devise a digital filter in which the delay is an analogue component, used to stagger the clocks of two analogue-to-digital convertors sampling at the Nyquist rate, for example.

A mapping has been derived between the jammer's angle of incidence from boresight and the maximum phase-shift required at band-edge relative to that at centre frequency. As the angle of incidence increases in either direction from boresight, the modulus of the filter's second weight must be increased from zero to achieve the appropriate phase-shift at band-edge. However, because of the necessary limit on intertap delay described above, and a practical limit on the weight modulus, the maximum phase-shift across the band is limited and so therefore is the angular sector over which nulling can be achieved. The size of the sector depends on the dimensions of the antenna system. For BYSON, it is 55˚ either side of boresight, although repositioning of the auxiliary horn could lead to adequate performance at all azimuths. For smaller-geometry systems, adequate nulling might be achieved over a sector wider than the real azimuth-space, in which case the intertap delay could be increased beyond the recommended maximum and the variation of weight-modulus reduced accordingly. It should be noted, incidentally, that a large modulus of the second weight would not necessarily lead to increased thermal noise transmission because the modulus of the first weight would be reduced to make the overall gain of the auxiliary channel match that of the main in the direction of jamming. The overall auxiliary gain would determine the amount of noise injected into the output.

The analysis methods used in this report can be applied only to simple systems. If, for example, a system with more filter taps were to be analysed, Fourier transform methods would be more appropriate. One issue to pursue is whether increasing the

15

number of taps allows a longer intertap delay to be used, perhaps even the Nyquist sampling interval in the limit. Since Nyquist samples in principle contain all the information about a signal, it should be possible to use these alone to synthesise the signals with the smaller time-difference required by the two-tap filter. It should be possible to derive the number of such samples required.

Even for simple systems, the analysis methods here must be used for quantitative results with caution because they separate the effects of amplitude and phase mismatch between main and auxiliary channels. In practice, the adaptive processor minimises jammer power at the output of the SLC by a combined adjustment of the auxiliary's amplitude and phase response.

Finally, the variation of relative phase with frequency between the channels analysed here and illustrated by the phase-difference surface only takes into account dispersion due to the electrical spacing of the main and auxiliary horns Other effects can add to the variation. The use of a transversal filter to compensate for the additional variation due to multipath has been examined by Morgan and Aridgides [5], who conclude that a large number of taps may be required, again separated by considerably less than the Nyquist interval. A further variation may be due simply to mismatches in the frequency response of the two channels. It seems inappropriate to apply an adaptive filter to correct these, when occasional calibration should be adequate.

5   REFERENCES

1   Howells P. W. "Explorations in fixed and adaptive resolution at GE and SURC", IEEE Trans. Antennas and Propagation, Vol. AP-24, No. 5, Sep. 1976, pp. 575-584.

2   Hudson J. E. "Adaptive Array Principles", Peter Peregrinus, 1981 or 1989.

3   McWhirter J. G. "A brief review of adaptive null steering techniques", RSRE Memorandum No. 3939, Feb. 1986.

4   Scott K. K. "Transversal filter techniques for adaptive array applications", Proc. IEE, Vol. 130, Part F or H, No. 1, Feb 1983, pp. 29-35.

5   Morgan D. R. and Aridgides A. "Adaptive sidelobe cancellation of wideband multipath interference", IEEF Trans. Antennas and Propagation, Vol. AP-33, No. 8, Aug 1985, pp.908-917.
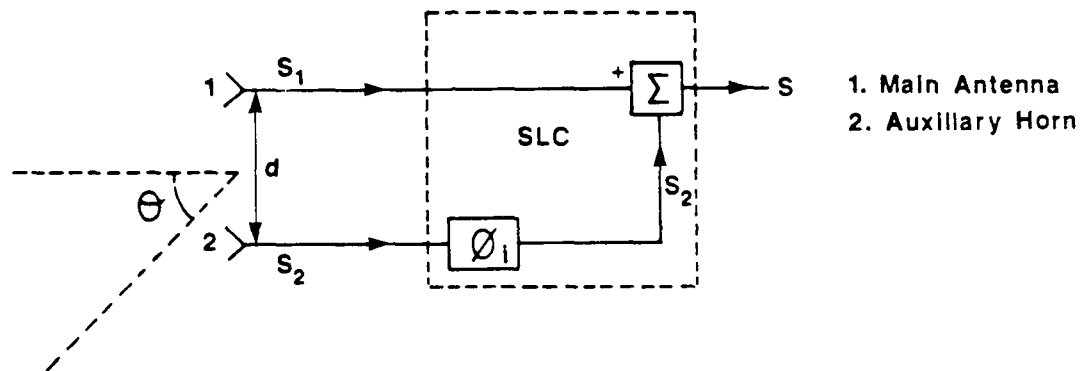
FIGURE 1 Simple SLC with one degree of freedom.
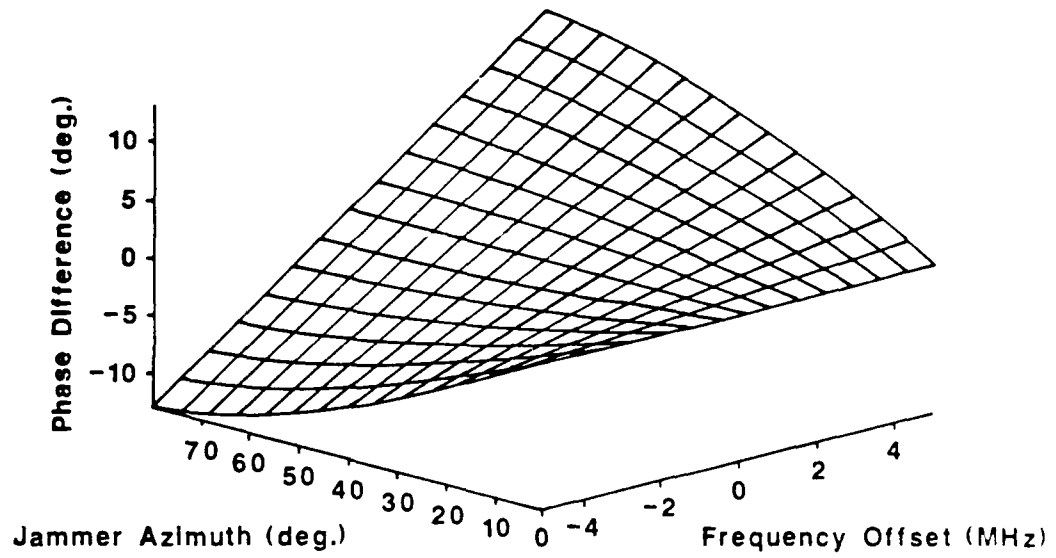
FIGURE 2 Phase-difference surface for simple SLC.

1. Main Horn
2. Auxillary Horn
3. Reflector
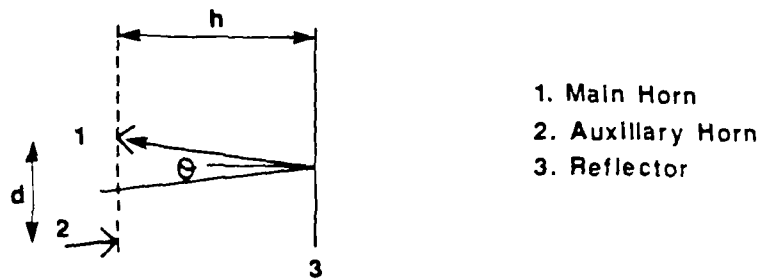
FIGURE 3a Plan view of a practical SLC antenna-arrangement
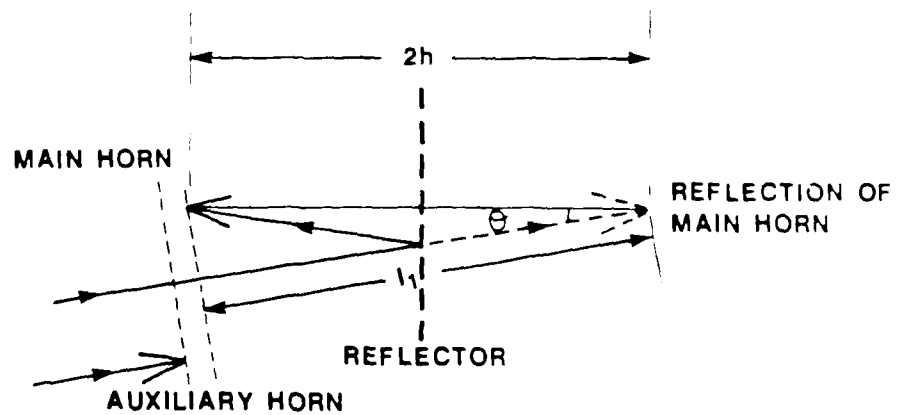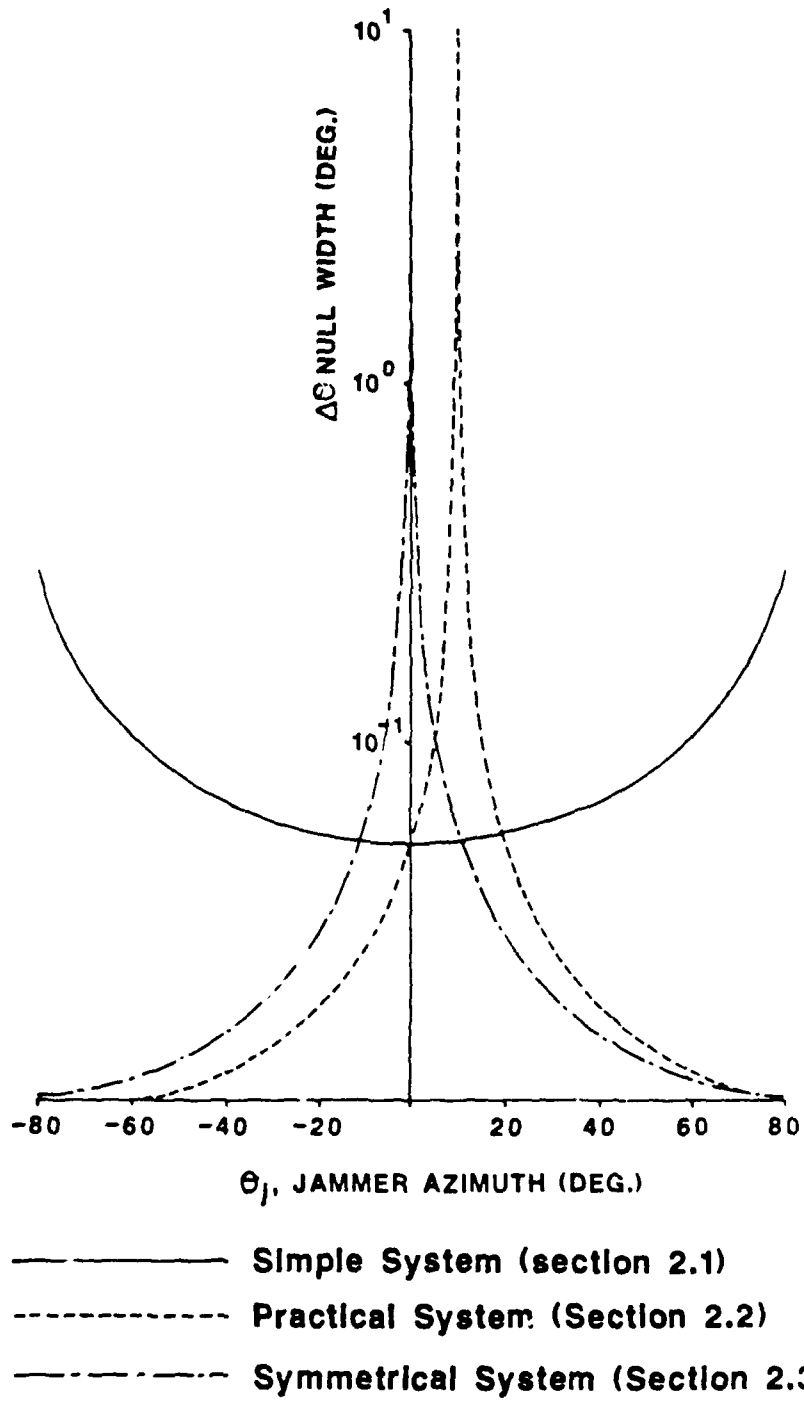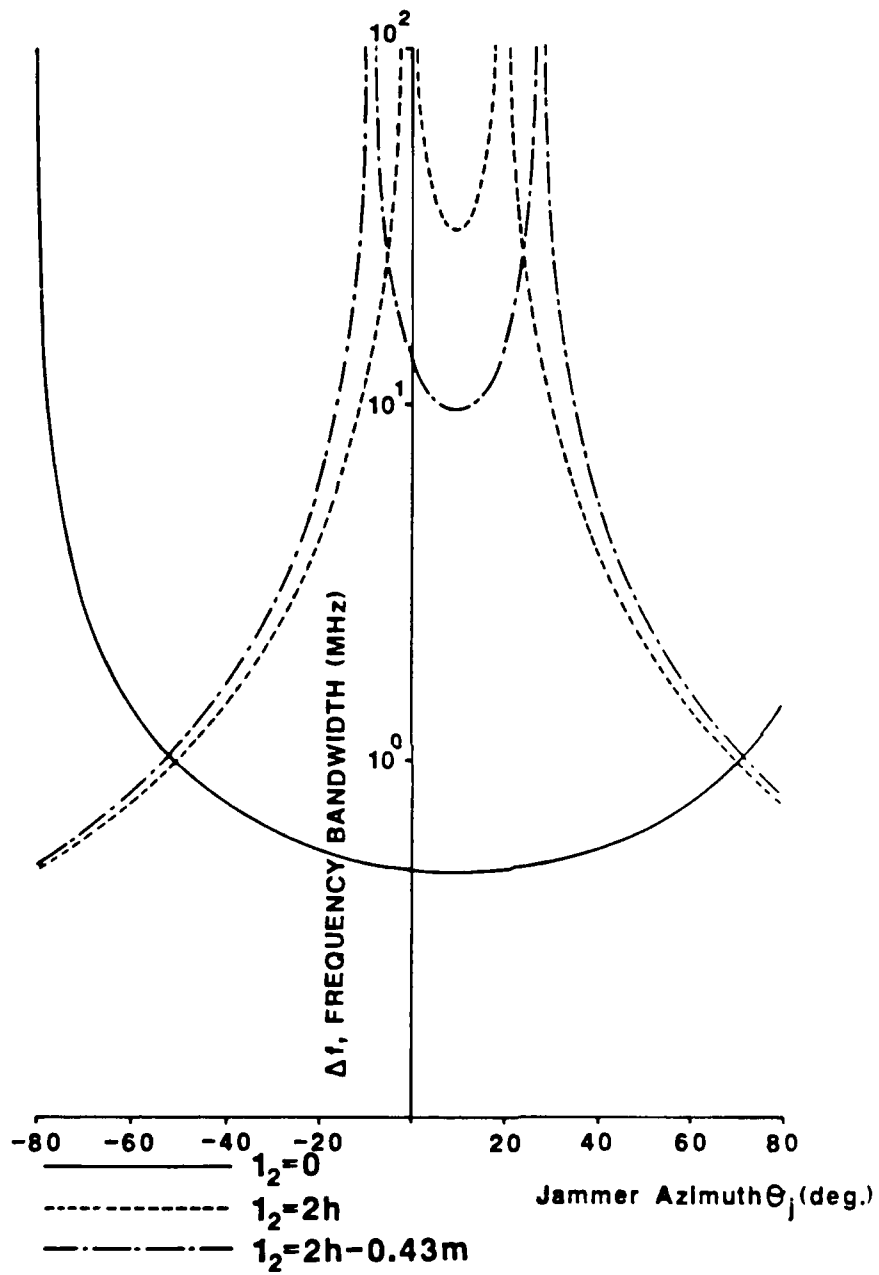

FIGURE 3b Rearranged plan view of practical SLC.
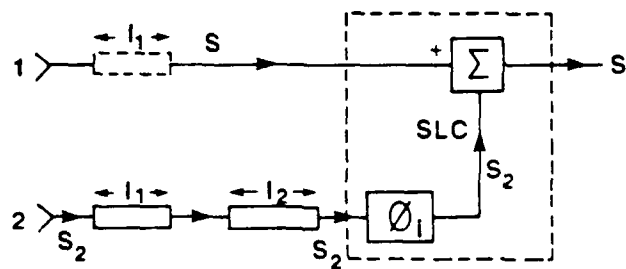
FIGURE 4 Schematic model of practical SLC.

FIGURE 5 Angular width of null for various SLCs based on BYSON.

FIGURE 6 Frequency bandwidth of null for BYSON SLC
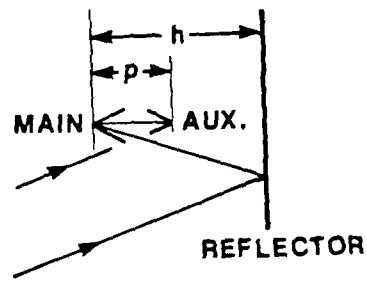with various lengths of compensating delay-line.

FIGURE 7a Plan view of practical SLC with symmetry
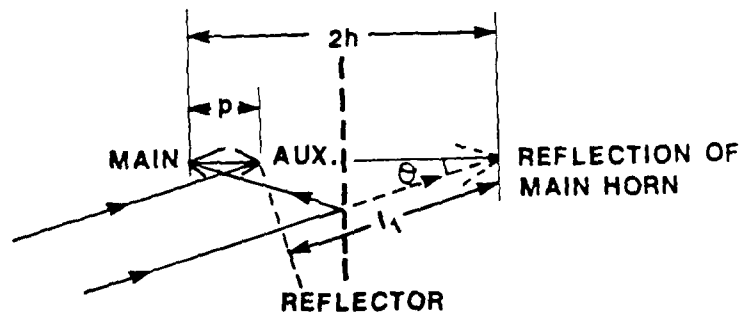
FIGURE 7b Rearranged plan view of practical SLC with symmetry
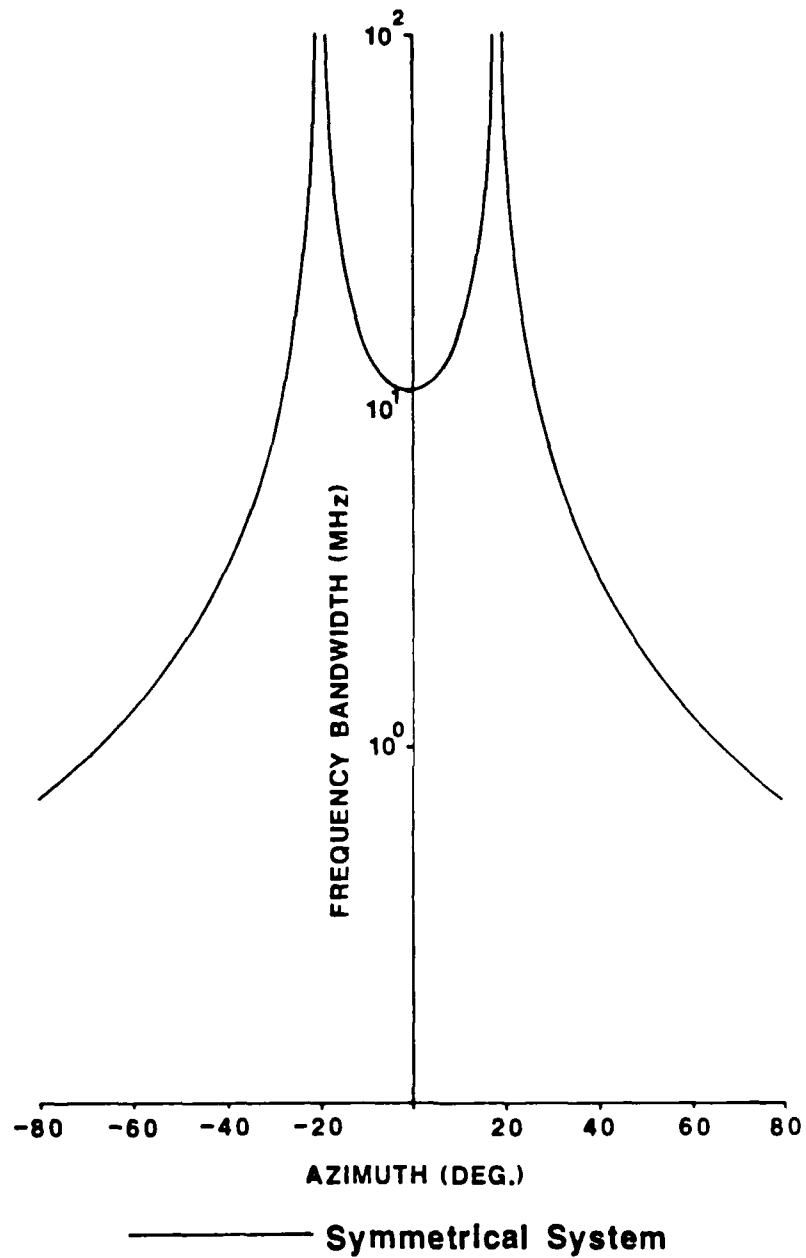
FIGURE 8 Frequency bandwidth of null for BYSON SLC
with symmetry.
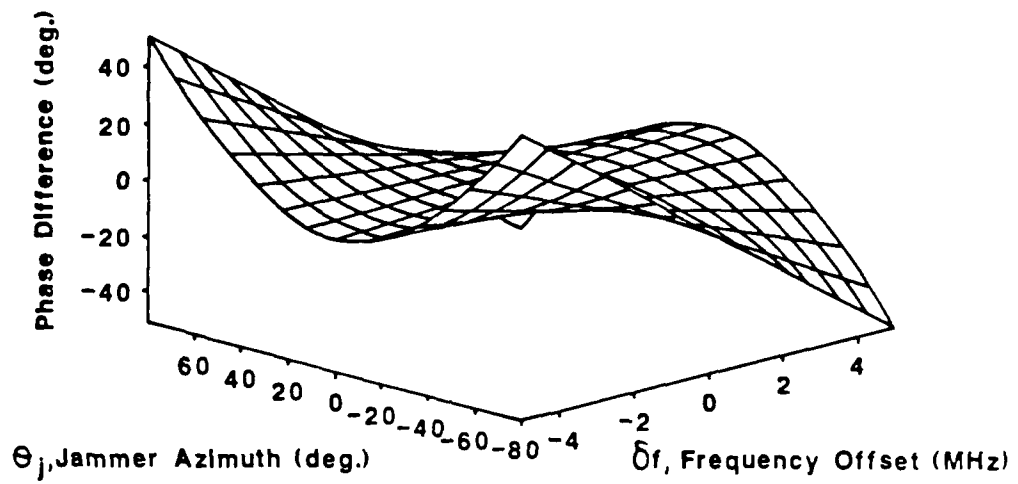
FIGURE 9 Phase-difference surface for BYSON SLC
with symmetry.
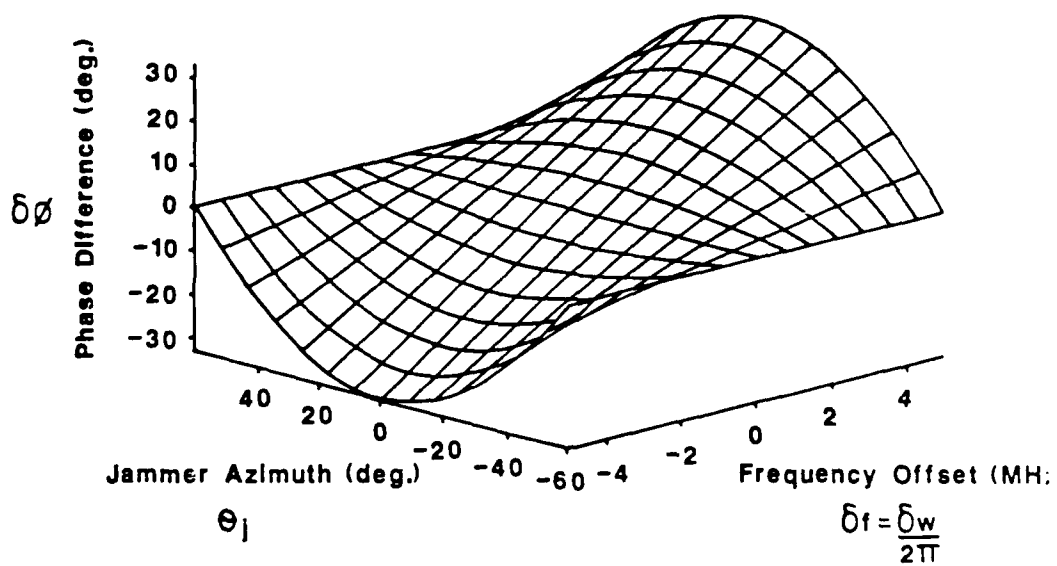
FIGURE 10 Rotated phase-difference surface with everywhere a **positive slope** with frequency.
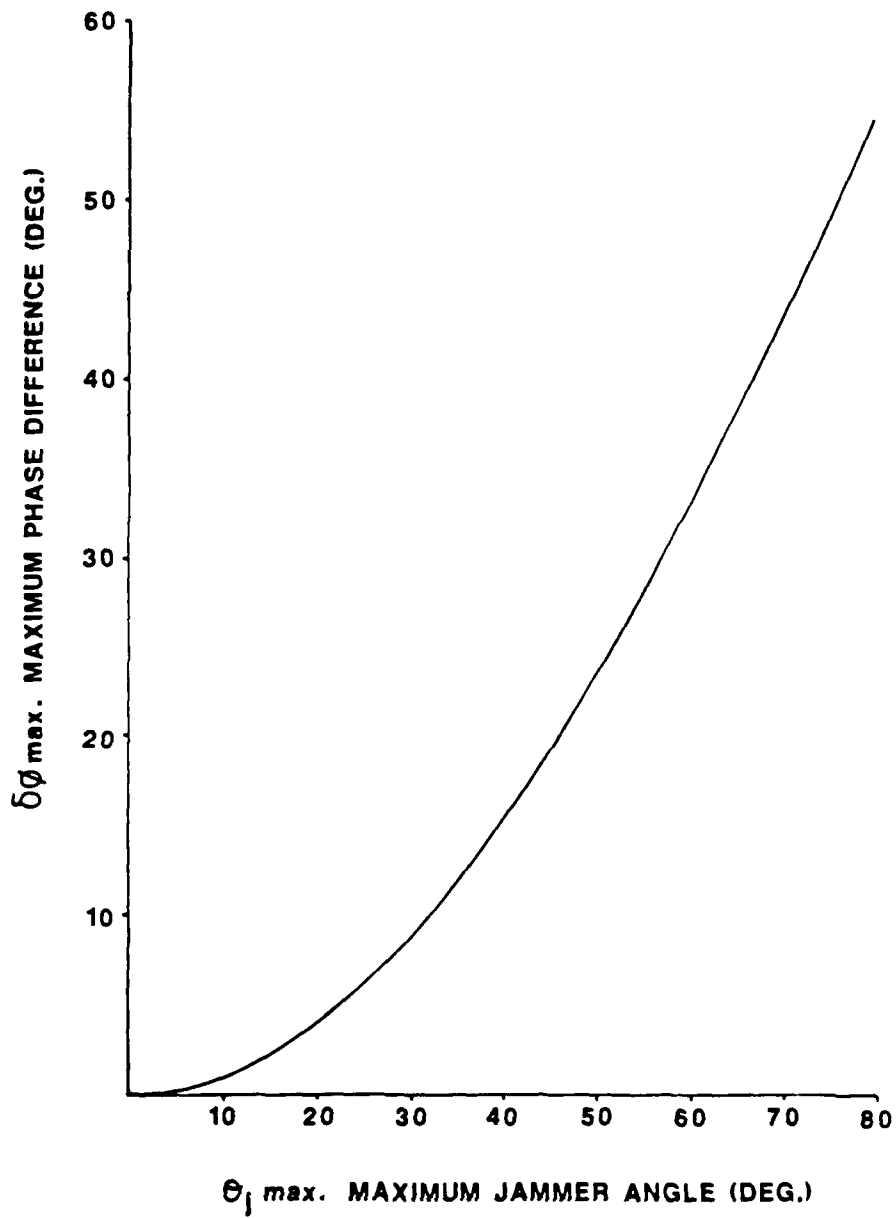
FIGURE 11 Maximum phase difference at 5 MHz from
band-centre relative to band-centre for a symmetrical
BYSON SLC.
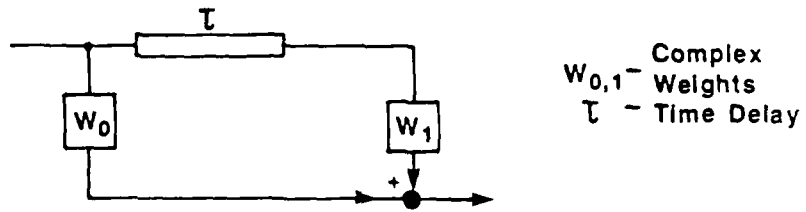
FIGURE 12 Transversal-filter schematic.
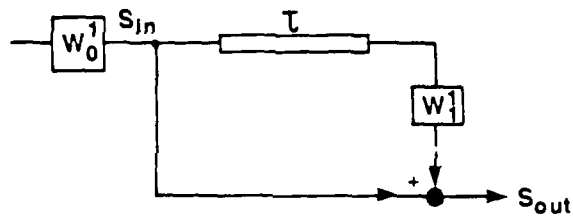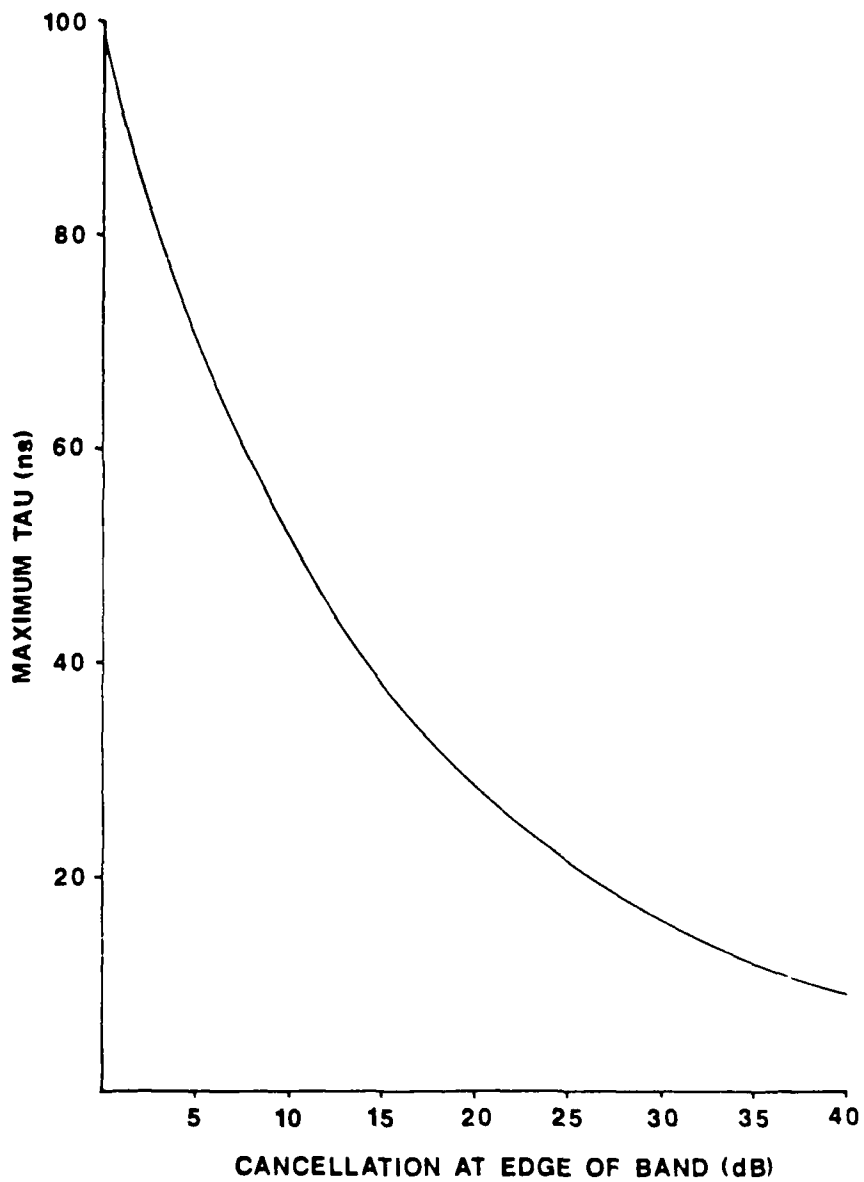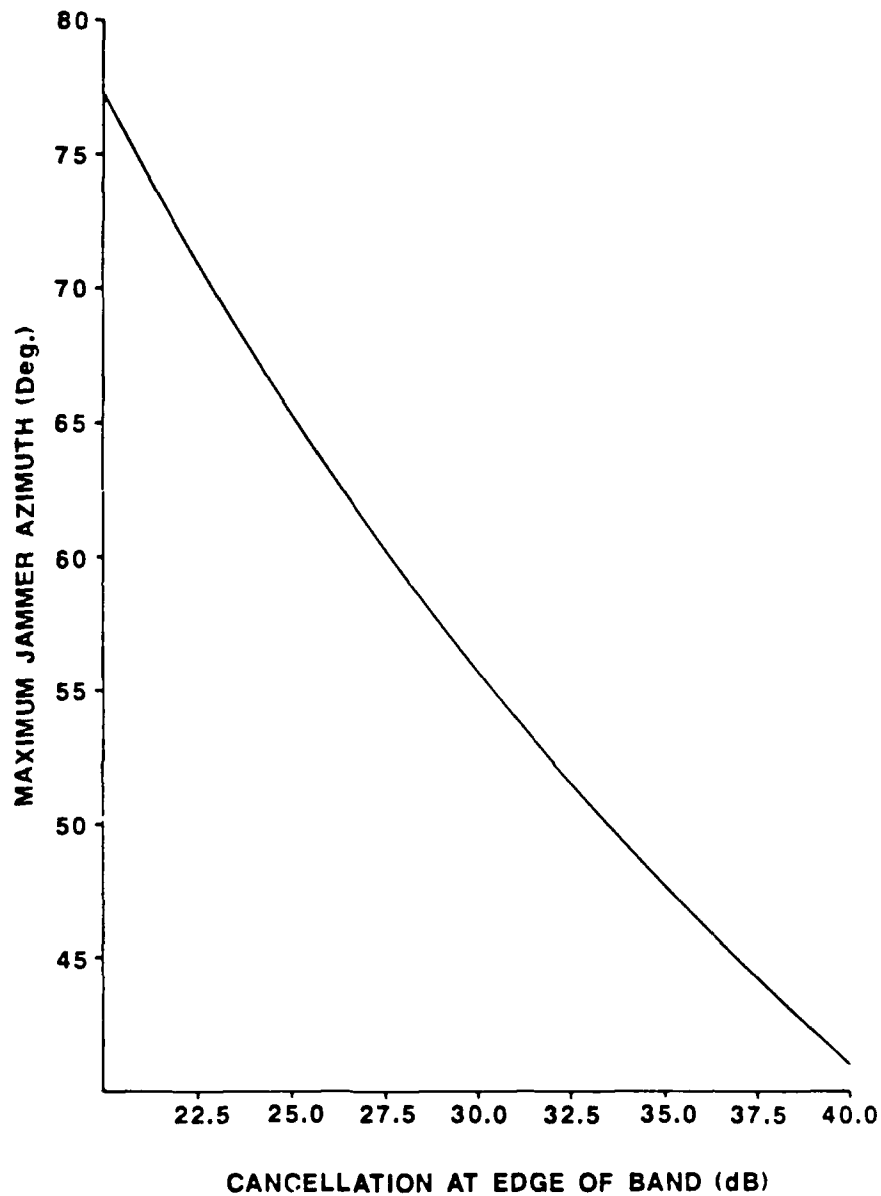

FIGURE 13 Rearranged transversal-filter schematic.
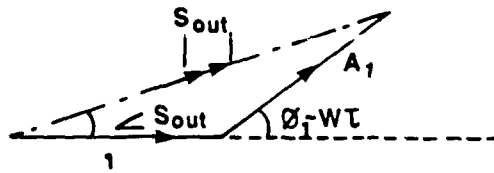

FIGURE 14 Phasor diagram for second part of transversal filter.
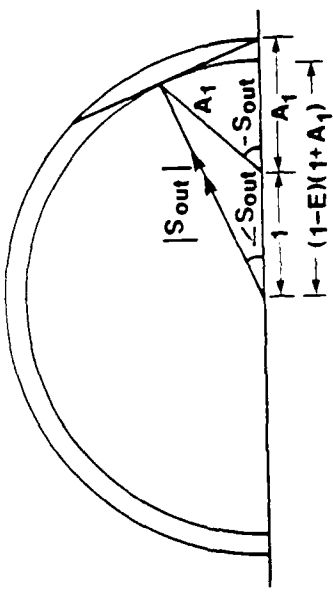
FIGURE 15 Phasor diagram for investigating the effect of weight modulus and intertap delay on the filter response.

FIGURE 16 Maximum intertap delay, determined by the
minimum cancellation acceptable at the edge of the band.

FIGURE 17 Illustrating the size of the sector either side of boresight over which jamming can be cancelled in BYSON with a specified performance at band-edge.
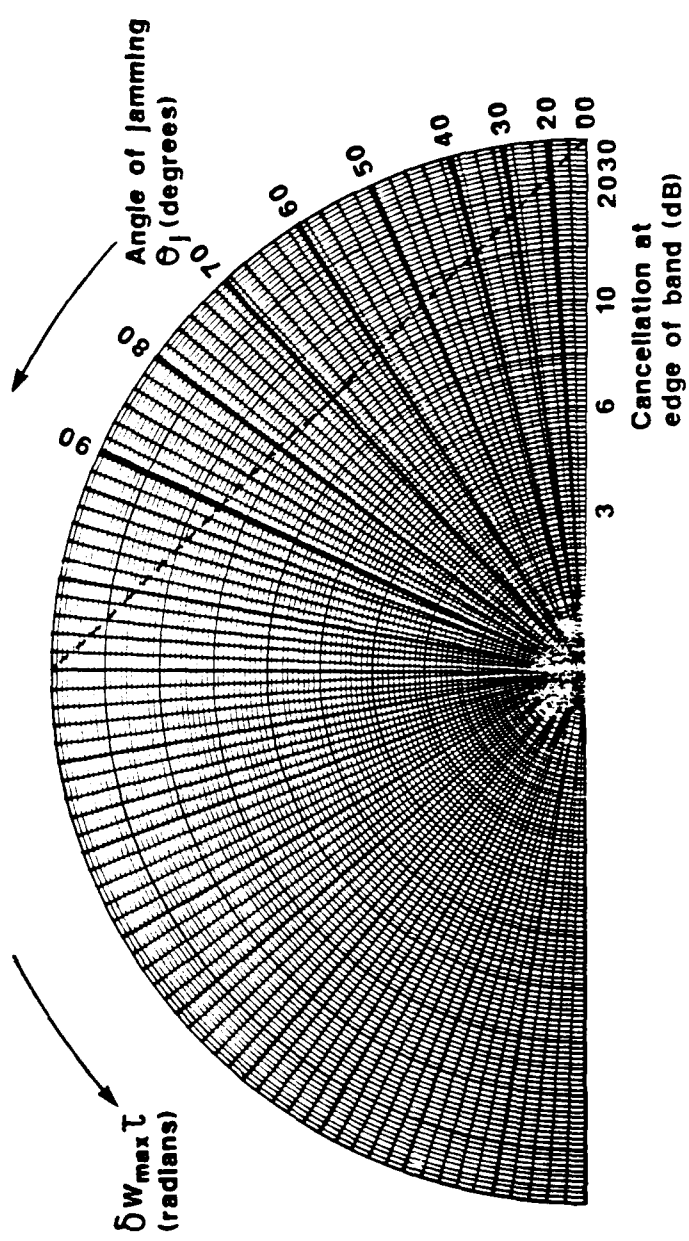
FIGURE 18 Polar diagram for investigating the effect of intertap delay on the cancellation at band-ecge obtained for different jamming angles.

REPORT DOCUMENTATION PAGE

DRIC Reference Number (If known) ....

Originators Reference/Report No.	Month	Year
MEMO 4375	AUGUST	1990

Originators Name and Location

RSRE, St Andrews Road
Malvern, Worcs WR14 3PS

Monitoring Agency Name and Location

Title

ANALYSIS OF THE PERFORMANCE OF A
SINGLE-AUXILIARY SIDELOBE CANCELLER

Report Security Classification	Title Classification (U, R, C or S)
UNCLASSIFIED	U

Foreign Language Title (in the case of translations)

Conference Details

Agency Reference	Contract Number and Period
Project Number	**Other References**

Authors	Pagination and Ref
DAY, I; FAIRHEAD, A C	32

Abstract

A geometrical approach to analysing the performance of simple sidelobe canceller systems is illustrated Systems with a single degree of freedom and with a two-tap transversal filter are analysed Throughout, examples are given based on RSRE's BYSON antenna. These show that a single auxiliary channel containing a two-tap transversal filter allows jamming arriving from any azimuth to be nulled over the radar-signal bandwidth. More general results may be deduced from the analysis

	Abstract Classification (U,R,C or S)
	U

Descriptors

THIS PAGE IS LEFT BLANK INTENTIONALLY